Nondestructive Testing and Evaluation
Vol. 00, No. 00, March 2008, 1–10

GUIDE

Piezoelectric radiofrequency transducers as passive buried sensors

T. Rétornaz[a], J.-M Friedt[a*], S. Alzuaga[b], T. Baron[b], É. Lebrasseur[b], G. Martin[b], T. Laroche[b], S. Ballandras[b,a], M. Griselin[c], J.-P. Simonnet[d]

[a]*SENSeOR SAS, Besançon, France*; [b]*Institut FEMTO-ST, UMR CNRS 6174, Time & Frequency department, Besançon, France* [c]*Lab. ThéMA, UMR CNRS 6049, Besançon, France* [d]*Lab. Chrono-Environnement, UMR CNRS 6249, Besançon, France*

(*summer 2011*)

We demonstrate that single-piezoelectric substrate based acoustic transducers act as ideal sensors for probing with various RADAR strategies. Because these sensors are intrinsically passive devices working in the radiofrequency range, they exhibit improved interrogation range and robustness with respect to silicon-based radiofrequency identification tags. Both wideband (acoustic delay lines) and narrowband (acoustic resonators) **transducers** are shown to be compatible with pulse-mode and frequency-modulated continuous-wave RADAR strategies respectively. We particularly focus on the Ground Penetrating RADAR (GPR) application in which the lack of local energy source makes these sensors suitable candidates for buried applications in roads, building or civil engineering monitoring. A novel acoustic sensor concept – High-overtone Bulk Acoustic Resonator – is especially suited as sensor interrogated by a wide range of antenna set, as demonstrated with GPR units working in the 100 and 200 MHz range.

Keywords: Ground Penetrating RADAR; acoustic wave sensor; piezoelectric substrate; wireless interrogation; passive sensor; HBAR;

1. Introduction

Ground Penetrating RADAR (GPR) is a classical tool for non-destructive observation of buried structures and interfaces, both for geophysical purposes or civil engineering [1] and road aging assesment [2–4]. More generally, various RADAR strategies are used for monitoring liquid and granualar media level [5, 6] or target velocities. In such uses, the measurement is limited to electromagnetic wave reflection by dielectric permittivity or conductivity interfaces.

We aim here to demonstrate how Acoustic Wave sensors provide an ideal match to classical RADAR measurement techniques in order to provide passive sensors interrogated through a wireless link [7, 8]. Surface Acoustic Wave (SAW) [9] sensors have been demonstrated as transducers for temperature [10–15], stress [16], torque [17], pressure [18–20] and chemisorption monitoring [21–23] as well as for tagging (identification only) applications [24–26]. However, since such devices will only work in a given restricted frequency range compatible with a given RADAR geometry, we extend the demonstration from SAW to a novel Bulk Acoustic Wave (BAW) resonator configuration operating in a wide frequency range and hence compatible

*Corresponding author. Email: jmfriedt@femto-st.fr

ISSN: 1058-9759 print/ISSN 1477-2671 online

DOI: 10.1080/10589750xxxxxxxxxxxxx
http://www.informaworld.com

with multiple RADAR antenna geometries. We specifically focus on the application of buried sensors interrogated by GPR – with an experimental demonstration using a pulse mode RADAR and discussion of the Frequency Modulated Continuous Wave (FMCW) and Frequency-Step Continuous Wave (FSCW) configurations.

The next section will briefly describe RADAR basics and focus on GPR. Section 3 will summarize the main characteristics of acoustic transducers, while the following sections will aim at demonstrating **the use of both kinds of RADARs targetted to probing the reponse of** delay lines (section 3), resonators (section 4) and the novel HBAR transducer (section 6).

2. Ground Penetrating RADAR basic principle.

Classical GPR instrumentation is characterized by two main operation modes: the wideband pulse mode GPR and narrowband FMCW and FSCW.

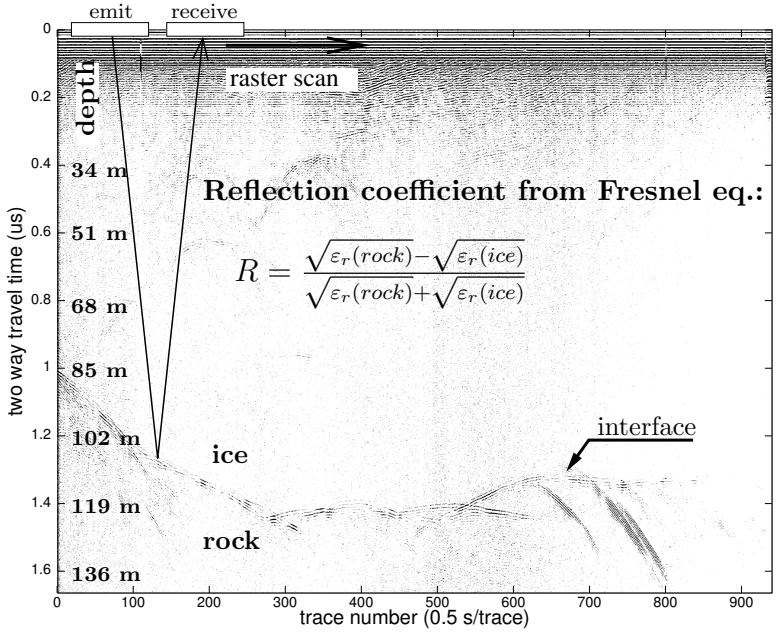

Figure 1. Radargram of a glacier acquired using 100 MHz dipole antennas. The reflection coefficient of an electromagnetic wave generated in a bistatic configuration, reaching in this example the ice-rock interface, is given by the Fresnel equation in the far field approximation. In a low conductivity medium such as dry ice, the interrogation range is defined by free-space propagation loss and reflection coefficient at the interface. Data recorded at Austre Lovénbreen, Svalbard, Norway

Pulse mode GPR generates a short – wideband – energetic pulse and requires fast sampling **of the returned signal**: either using an equivalent time sampling [27] strategy for low cost operation under the assumption of constant environmental conditions during the interrogation period (typically several tens of milliseconds), or baseband sampling thanks to recent fast A/D converters following the Software Defined Radio (SDR) approach. The pulse width is defined by the antenna impedance, which is itself related to the antenna dimensions and dielectric properties of the surrounding medium. Hence, pulse-mode GPR will not generate a pulse centered on a known frequency but **operates** at a given wavenlength defined by the dimensions of the emitting antenna. In such a configuration, for frequencies below 3 GHz, a capacitor is loaded with a high voltage and transfers radiated energy as a

brief pulse thanks to an avalanche transistor whose current v.s voltage characteristics is defined by a positive feedback loop. For a low enough intrinsinc capacitance, the characteristic time needed to empty the high-voltage capacitor as radiated energy is defined by the resonance frequency of the antenna. Thus, the time constant can widely vary whether the antenna is surrounded by low **permittivity** media (ice) or a high permittivity environment (liquid water or water saturated sand for example). This condition will become a significant hindrance when using a pulse mode GPR to probe narrowband resonators which might become out of band when the GPR is used over unsuitable media.

In an FMCW – or the related Frequency Step Continuous Wave (FSCW) – a continuous radiofrequency wave is emitted from one antenna. Either a low-frequency signal is recovered at a beat frequency proportional to the distance of the reflector (FMCW), or both phase and magnitude of the returned signals are recovered through I/Q demodulation in case of a FSCW. Both strategies provide the needed information to either recover time domain information representative of the stratigraphy of the environment through an inverse Fourier transform under the basic assumption of a constant permittivity of the media through which the electromagnetic waves propagate, or through more complex analysis of dispersive media **if** both permittivity and reflector depth are identified [28].

Considering the dielectric properties of the homogeneous materials on both sides of an interface are known, the reflection coefficient of the electromagnetic wave is **known** from Fresnel equation under the far-field assumption (plane wave reaching the interface): this reflection coefficient will be compared with the reflection coefficient of the sensor we wish to probe using a GPR (Fig. 1).

3. Surface Acoustic Wave delay line basic princple and interrogation strategies

Surface Acoustic Wave (SAW) transducers are based on the conversion of an incoming electromagnetic wave to a mechanical wave (inverse piezoelectric effect) propagating at the air-substrate interface, and then converted back as an electromagnetic wave (direct piezoelectric effect) returned to the reception antenna [29]. As such, the SAW transducer appears as a 2-port electrical component, but understanding the underlying measurement principle is mandatory for proper design of the SAW in a sensing application. Since physical conditions of the environment of the transducer induce a change in the acoustic velocity of the mechanical wave propagating on the single-crystal piezoelectric substrate, the reflective radiofrequency properties of the electric dipole (S_{11} measurement) are indicators of these physical conditions. Under appropriate design conditions, one physical quantity will yield a dominant response with respect to other effects. In order to either perform multiple measurements or decorrelate the contribution of each physical quantity – including the distance of the RADAR antenna to the sensor – a differential approach is used.

The most common SAW sensor configuration is the SAW tag, a wideband device excited by a short electromagnetic pulse and whose returned information is a series of pulses: the number of returned pulses is defined by the number of mirrors patterned through cleanroom lithography techniques on the piezoelectric substrate. For sensing application only a few mirrors are needed (at least two, one for the reference pulse and the other for the measurement). Coding has been demonstrated with a large number of bits, with over 20 mirrors patterned on the substrate [26]. Since the reflected pulse time interval only provides a rough estimate of the physical quantity due to the minute velocity changes associated with the transducer environment property change, a phase subtraction between successive pulses

is classically used to provide a precise measurement of the acoustic velocity and hence physical quantity (Fig. 2) [30]. Such a measurement requires either both the returned magnitude *and phase* informations or, as provided by GPR, a baseband measurement of the returned power. Since baseband sampling at several times the central frequency – sampling at 500 to 40000 MHz for central frequencies typically in the 50 to 1500 MHz range – is technically challenging and hardly compatible with embedded, low power designs [31], an equivalent time sampling assuming a slowly varying environment of the refectors is often used. In such a strategy, N successive measurements are performed at times $N \times \Delta\tau$ after the excitation pulse is emitted, yielding a series of N samples separated by a time interval $\Delta\tau$ or an equivalent sampling rate of $1/\Delta\tau$. Hence, the challenge of sampling at 40 Gsamples/s is replaced with a slow analog-to-digital converter measuring the voltage recorded by a fast sample-and-hold with 25 ps accuracy (7.5 mm-long transmission line in vacuum). Typical time-domain reflections are in the 1 to 5 μs range since the acoustic velocity is typically in the 3000 to 5000 m/s depending on the piezoelectric substrate and the kind of acoustic wave propagating, yielding sensors with dimensions in the centimeter range (a 5 μs delay at 5000 m/s requires a 1.25 mm long acoustic path). 5 μs is a typical measurement interval for GPR associated with a 425 m deep interface in ice for example (the electromagnetic velocity in ice is assumed to be 170 m/μs in this example [32]), beyond the typical attenuation range of the electromagnetic pulse.

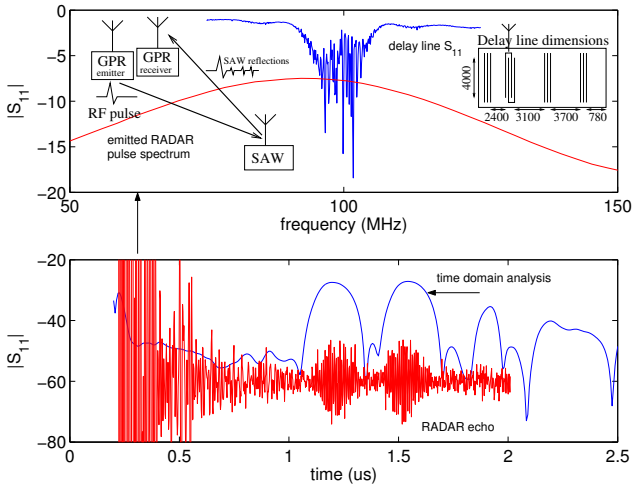

Figure 2. Top: experimental frequency domain characterization of the 100-MHz Malå RAMAC GPR pulse (red) and transfer function of a SAW delay line (blue) – schematic of the delay line with all dimensions in μm. Bottom: time domain signal returned by the SAW when probed using a GPR (red) and network analyzer characterization by inverse Fourier transform of the frequency-domain characterization (blue).

In an alternative configuration, the acoustic wave is confined between two Bragg mirrors, providing energy confinement conditions consistent with a narrowband transfer function, or in terms of time domain analysis a long energy dissipation time. In such a configuration, the usable returned signal is no longer a time delay but a frequency, since such a resonator acts as a narrowband transducer. Resonators are poorly suited to pulse mode GPR interrogation since the short sampling duration (typically 5 μs at most) is hardly compatible with an accurate returned signal frequency identification. Indeed, piezoelectric single crystal substrates exhibit for temperature sensing a maximum sensitivity of 100 ppm, so that the frequency of a 100 MHz transducer must be identified with 10 kHz accuracy for 1 K accurate temperature measurements. Such an accuracy would require at least a 100 μs-long

record based on basic Fourier transform, or a 20-fold in the frequency identification improvement of the 5 μs long record if some assumption (single returned frequency) is made [33]. Furthermore, we have observed that the time-reference of pulse mode GPR hardly provides the needed accuracy for such a precise frequency measurement, and a differential (two resonance frequency identification) approach is mandatory to get rid of delay line aging and drift, as well as sensor aging and electromagnetic envionmental variations (impedance pulling of the frequency). On the other hand, dedicated interrogation hardware has been developed for probing such narrwoband sensors with excellent resolution [34], which happens to work following principles similar to FMCW GPR [35, 36]. Actually, FMCW has been demonstrated as an excellent strategy for probing resonators acting as temperature sensors [34].

We demonstrate [8] that assuming the interrogation range of a GPR under given conditions is known – based on radargrams recorded at interfaces with reflection coefficient $IL_{ice-rock}$ (e.g. ice-rock interface in our case) – and considering the insertion loss IL_{SAW} of a SAW sensor is known, then the distance d_{SAW} at which a sensor can be interrogated is given by

$$d_{SAW} = d_{ice-rock} \times 10^{(IL_{ice-rock} - IL_{SAW})/40}$$

Using typical constants of a reflection coefficient at the ice-rock interface of -19 dB (assuming a relative permittivity of ice of 3.1 and 5 for rock) and insertion losses of -35 dB for a SAW delay line, then the interrogation range of a sensor is 0.4 times that **found for** the ice-rock interface. Considering we are able to gather a usable signal for ice-rock interfaces deeper than 100 m, the SAW sensor should be readable at a depth of at least 40 m. Experimental data were gathered with a sensor buried 5 m deep in snow, exhibiting a signal to noise ratio consistent with a 40 m maximum depth interrogation range [8]. **Acoustic sensor data analysis when probed by GPR only requires software signal processing, and no hardware modification:**

(1) a Fourier transform on the returned signal radargram (Fig. 3, bottom-left) identifies whether a sensor is located within the RADAR interrogation range (Fig. 3, top-right),

(2) for each trace (Fig. 3, bottom-right) in which a frequency-signature of the sensor is identified (Fig. 3, top-left), the phase of the Fourier component including most of the power is indicative of the acoustic delay, and hence of the physical quantity under investigation.

4. Probing Resonators with Ground Penetrating RADAR

Pulse mode GPR are intrinsically wideband devices hardly compliant with most radiofrequency regulations, but acceptable for geophysical applications. The antenna size – and hence central frequency of the emitted pulse – is usually selected as a tradeoff between depth resolution (the higher the frequency, the better the resolution) and penetration distance of the electomagnetic wave (the lower the frequency, the deeper the reflected signal which can be detected). Hence, an associated sensor must adapt to the available frequency range of common GPR – typically in the 50 to 1500 MHz range. Although acoustic delay lines are wideband devices, a given sensor will nevertheless only be compatible with a single antenna (100, 200, 400 MHz or above range).

SAW delay i**lines** are 500 μm-thick, 1 cm^2-large sensors : the associated antenna

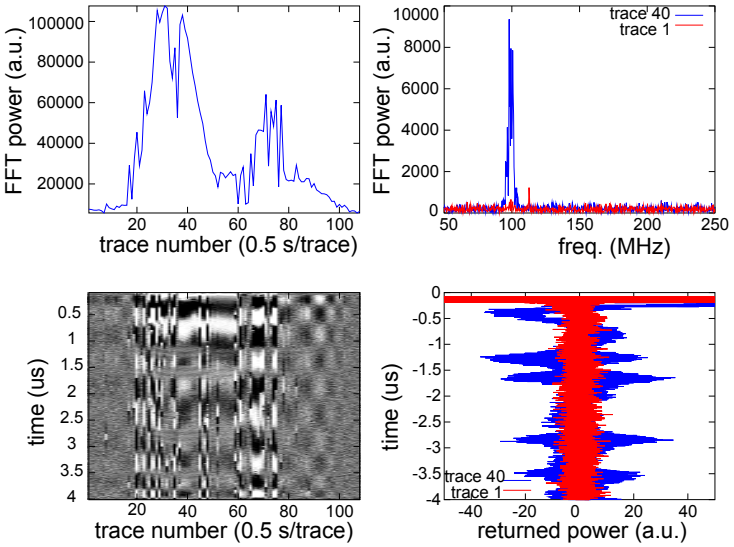

Figure 3. Processing steps for identifying the sensor signal: bottom left, the raw radargram acquired using a 100 MHz antenna set, two way trip over a 100 MHz delay line acting as a sensor. An 11-th order polynomial fit was removed from each trace to reduce low-frequency background fluctuations from one trace to another. Top-right: magnitude of the Fourier transform of the recorded signal, excluding the emitted pulse, exhibiting the returned signal at 100 MHz when the sensor is visible (blue, trace 40) and invisible (red, trace 1). While the magnitude of the Fourier transform is the most visual indicator of the sensor detection, the phase of the Fourier transform at the maximum returned power frequency is the most accurate signature for quantitative information retrieval. Bottom-right: comparison of the time domain reflected signal when the sensor is visible (blue, trace 40) and absent (red, trace 1). Top-left: the integral of the magnitude of the Fourier transform of the returned power in the 95-105 MHz band is an indicator of the presence of the sensor (the RADAR is located over the sensor at traces 30 and 55).

must be much larger to be efficient at the incoming electromagnetic wavelength. Although the dipole-length is reduced thanks to the high relative permittivity of the medium in which the sensor is buried, the antenna dimension nevertheless remains in the tens of **centimeters** length. A linear polarization of the antenna connected to the sensor – as provided by the most simple geometry of the dipole antenna – also means that the ground based interrogation GPR must be oriented accordingly so that the buried and surface dipoles are parallel. We have experimentally observed that in a crossed-polarization configuration, the returned power is too low to allow for a useful measurement, meaning that multiple sensors can be located in common view of the GPR and selected through surface antenna orientation during the measurement.

5. Sensor signal identification

Using the same instrument to probe both the buried dielectric and conductivity interfaces and sensor signal yields the issue of classifying which reflection is associated with which phenomenom. **In case of the pulse mode GPR, two criteria allow for the identification of a sensor signal (Fig. 4)**:

(1) the design of SAW delay line typically locates the first reflection at least 1 μs after the incoming electromagnetic pulse reaches the sensor. Such a delay (500 ns two-way trip) would be associated with an interface located 42 m deep in ice or 7.5 m deep in water. The signal to noise ratio of the reflected signal, associated with a sensor shallower than expected from an electromagnetic propagation, will obviously allow the association of the

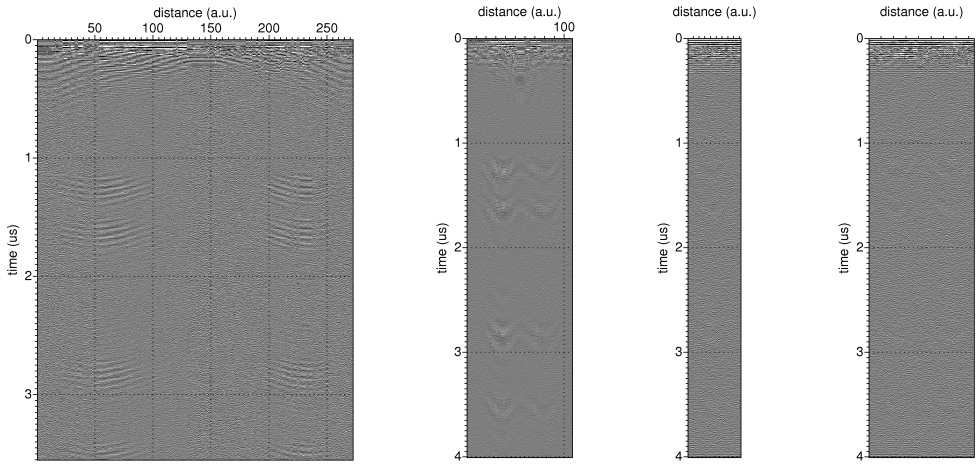

Figure 4. Left to right: two examples of 100 MHz delay line probed with a Malå RAMAC bistatic GPR connected to a 100 MHz dipole antenna (1261 MHz sampling frequency, 4487 and 5060 samples respectively); two examples of probing a 200 MHz delay line using a Malå RAMAC bistatic GPR connected two 200 MHz dipole antenna (1261 MHz sampling frequency, 5060 samples). The reflections from the sensor are located at delays 1.3 μs, 1.6 μs, 2.8 μs, and 3.5 μs. The first, second and fourth image depict two-way trips over the sensor, while the third image was acquired with only a one way trip over the sensor. All data processed with the Seismic Unix software.

returned signal to the sensor rather than to a buried interface. Such a classification step is similar to the time-domain multiplexing (TDMA) familiar to radiofrequency communications,

(2) during the migration post-processing step, the hyperbola curvature on which all points associated with a single point-like reflector lie is dependent on the reflector depth. Since the time delay due to a SAW delay line is associated with an acoustic velocity rather than the electromagnetic velocity, the curvature of the hyperbola on which the sensor-related echos lie will be that of a shallow reflector and the automated migration algorithm will not be able to focus all the data on a single point-like reflector.

In the case of narrowband reflectors, the quality factor of acoustic sensors – typically in the 10000 range below 400 MHz – is much larger than any natural reflector, even dielectric media located between parallel conducting plates acting as reflectors. Hence, the long (several microseconds) time-domain echo, or in the frequency domain the narrowband frequency definition of the returned signal, is hardly missed for a dielectric reflector.

6. Novel resonator design for use with Ground Penetrating RADAR

In order to provide a sensor configuration compatible with multiple antenna geometries, e.g. compatible with the frequency range 100 to 400 MHz, a frequency comb must be generated over this frequency range. One geometry which appears promising for such a purpose is the High Overtone Bulk Acoustic Resonator (HBAR) [37] configuration in which a bulk acoustic wave is confined inside a low-acoustic loss thick (300-500 μm) substrate, while the high operating frequency condition is defined by a thin ($<$ 100 μm) piezoelectric layer coated on the dielectric substrate. The broadband envelope of the transfer function (Fig. 5, left) – here with a maximum returned power around 200 MHz – is defined by the piezoelectric layer thickness, and the comb period (whether in time or frequency domain) by the thickness of the thick substrate. We have demonstrated high quality factor and wide frequency operation range with such a configuration (Fig. 5, right): the 1 mm$\times$1 mm HBAR is connected to 2$\times$40 cm enameled wire dipole antenna.

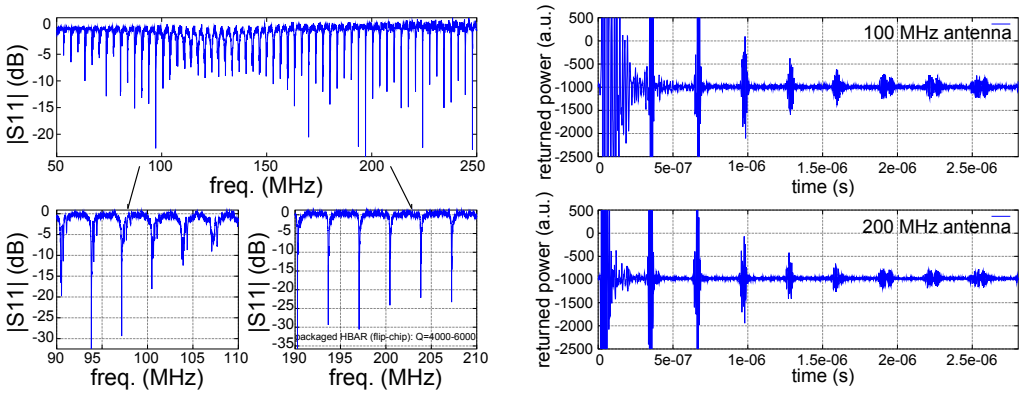

Figure 5. Left: frequency-domain characterization of an HBAR using a radiofrequency network analyzer (Rohde & Schwartz ZVL). Modes are separated by 3 MHz gaps (top: wideband characterization exhibiting the mode continuum from below 100 MHz to above 200 MHz; bottom-left: zoom around the 100 MHz area; bottom-right: zoom around the 200 MHz area). Right: time domain characterization of this same HBAR, with reflections appearing every 300 ns, performed using Malå RAMAC 100 MHz antenna (top) and 200 MHz antenna (bottom). Since the acoustic velocity of the wave changes with physical properties of the environment of the HBAR, the time delay between successive reflections is an indicator of such physical properties. This particular HBAR design exhibits little temperature coefficient of frequency, and hence little velocity dependence with temperature, providing useful tagging information.

7. Conclusion

Beyond the use of RADARs in general and GPR in particular for probing passive reflectors, we demonstrate that acoustic wave devices are perfectly suited as cooperative targets for monitoring physical quantities thanks to existing RADAR systems. Both wideband sensors – acoustic delay lines – and narrowband sensors – resonators – are suited for the various classical RADAR measurement strategies, namely pulse mode and frequency-modulated continuous wave measurements. The recorded signals require no modification of the hardware, and identifying the physical quantity under investigation only requires post-processing of the data to extract either an accurate time delay (as a phase between successive echos in the wideband strategy) or frequency (in the FMCW narrowband strategy), both of which are representative of the acoustic velocity in the sensor and hence the physical quantity affecting most significantly the sensor behaviour thanks to a design reducing the influence of unwanted velocity variation sources. Furthermore, a differential approach in which sensors with different behaviour to external disturbances are interrogated reduces the influence of correlated noise, aging and local time reference drift.

Acknowledgements

Part of the funding for this project was provided by the French National Research Agency (ANR) under the Cryo-Sensors grant.

References

[1] G. Clemena *Handbook on nondestructive testing of concrete, 2nd Ed.*, CRC Press, West Conshohocken, PA, USA, 2003.

[2] T. Saarenketo and T. Scullion, *Road evaluation with ground penetrating radar*, Journal of Applied Geophysics 43 (2000), pp. 119–138.

[3] National Research Council, Rexford M. Morey *Ground Penetrating Radar for Evaluating Subsurface Conditions for Transportation Facilities*, American Association of State Highway and Transportation Officials, National Cooperative Highway Research Program, Washington, DC, USA, 1998.

[4] K. Maser, *Condition Assessment of Transportation Infrastructure Using Ground-Penetrating Radar*, Jour. Of Infrastructure Systems 2 (1996), pp. 94–101.

[5] G. Brooker *Sensors and Signals*, Australian Centre for Field Robotics, University of Sydney, Australia, 2007.
[6] B. Lipták *Chap. 3: Level Measurement*, Vol. 1, CRC Press, Boca Raton, FL, USA, 2003.
[7] C. Allen, K. Shi, and R. Plumb, *The use of ground-penetrating radar with a cooperative target*, IEEE Transactions on Geoscience and Remote Sensing 5 (1998), pp. 1821–1825.
[8] J.M. Friedt, T. Rétornaz, S. Alzuaga, T. Baron, G. Martin, T. Laroche, S. Ballandras, M. Griselin, and J.P. Simonnet, *Surface Acoustic Wave Devices as Passive Buried Sensors*, Journal of Applied Physics 109 (2011), p. 034905.
[9] R. White and F. Voltmer, *Direct piezoelectric coupling to surface acoustic waves*, Applied Physics Letters 7 (1965), pp. 314–316.
[10] X.Q. Bao, W.B. V.V. Varadanan , and V. Varadan, *SAW temperature sensor and remote reading system*, in *IEEE Ultrasonics Symposium*, Denver, CO, USA, 1987, pp. 583–585.
[11] W. Buff, S. Klett, M. Rusko, J. Ehrenpfordt, and M. Goroli, *Passive remote sensing for temperature and pressure using SAW resonator devices*, IEEE Transactions on Ultrasonics, Ferroelectrics, and Frequency Control 45 (1998), pp. 1388–1392.
[12] G. Scholl, F. Schmidt, T. Ostertag, L. Reindl, H. Scherr, and U. Wolff, *Wireless passive SAW sensor systems for industrial and domestic applications*, in *IEEE International Frequency Control Symposium*, 1998, pp. 595–601.
[13] W. Bulst, G. Fischerauer, and L. Reindl, *State of the Art in Wireless Sensing with Surface Acoustic Waves*, IEEE Transactions on Industrial Electronics 48 (2001), pp. 265–271.
[14] L. Reindl and I. Shrena, *Wireless Measurement of Temperature Using Surface Acoustic Waves Sensors*, IEEE Transactions on Utrasonics, Ferroelectrics, and Frequency Control 51 (2004), pp. 1457–1463.
[15] S. Schuster, S. Scheiblhofer, L. Reindl, and A. Stelzer, *Performance Evaluation of Algorithms for SAW-Based Temperature Measurement*, IEEE Transactions on Utrasonics, Ferroelectrics, and Frequency Control 53 (2006), pp. 1177–1185.
[16] A. Pohl, R. Steindl, and L. Reindl, *The "Intelligent Tire" utilizing passive SAW sensors – mesurement of tire friction*, IEEE Transactions on Instrumentation and Measurement 48 (1999), pp. 1041–1046.
[17] J. Beckley, V. Kalinin, M. Lee, and K. Voliansky, *Non-contact torque senseor based on SAW resonators*, in *IEEE Int. Freq. Control Symposium and PDA Exhibition*, New Orleans, LA, USA, 2002, pp. 202–213.
[18] H. Scherr, G. Scholl, F. Seifert, and R. Weigel, *Quartz pressure sensor based on SAW reflective delay line*, in *IEEE Ultrasonics Symposium*, San Antonio, TX, USA, 1996, pp. 347–350.
[19] G. Bruckner, A. Stelzer, L. Maurer, J. Biniasch, L. Reindl, R. Teichmann, and R. Hauser, *A high-temperature stable SAW identification tag for a pressure sensor and a low-cost interrogation unit*, in *11th International Sensor Congress (SENSOR)*, Nuremberg, Germany, 2003, pp. 467–472.
[20] H. Oh, W. Wang, K. Lee, I. Park, and S. Yang, *Sensitivity improvement of wireless pressure sensor by incorporating a SAW reflective delay line*, International Journal on Smart Sensing and Intelligent Systems 1 (2008), pp. 940–954.
[21] Y. Dong, W. Cheng, S. Wang, Y. Li, and G. Feng, *A multi-resolution passive SAW chemical sensor*, Sensors and Actuators B 76 (2001), pp. 130–133.
[22] W. Seidel and T. Hesjedal, *Multi-frequence and multi-mode GHz surface acoustic wave sensor*, in *IEEE Ultrasonics symposium*, Honolulu, HI, USA, 2003, pp. 1408–1411.
[23] M. Dierkes and U. Hilleringmann, *Telemetric surface acoustic wave sensor for humidity*, Advances in Radio Science 1 (2003), pp. 131–133.
[24] A.Pohl, F.Seifert, L.Reindl, G.Scholl, T. Ostertag, and W.Pietsch, *Radio signals for SAW ID tags and sensors in strong electromagnetic interference*, in *IEEE Ultrasonics Symposium*, Cannes, France, 1994, pp. 195–198.
[25] L.Reindl, G.Scholl, T.Ostertag, W.Ruile, H. Scherr, C. Ruppel, and F.Schmidt, *Wireless remote identification and sensing with SAW Devices*, in *International Congress Sensor97*, May 13-15, , Nuremberg, Germany, 1997, pp. 161–166.
[26] C. Hartmann, *A Global SAW ID Tag with Large Data Capacity*, in *Proceedings of 2002 IEEE Ultrasonics Symposium*, Vol. 1, Munich, Germany, 2002, pp. 65–69.
[27] J. Han, R. Xu, and C. Nguyen, 2007, On the development of a low-cost, compact planar integrated-circuit sampling receiver for UWB systems. in *Ultra-Wideband, Short-Pulse Electromagnetics 8* Springer, New York, NY, USA, pp. 161–170.
[28] H.P. Marshall and G. Koh, *FMCW radars for snow research*, Cold Regions Science and Technology 52 (2008), pp. 118–131.
[29] V. Plessky and L. Reindl, *Review on SAW RFID tags*, IEEE Transactions on Ultrasonics, Ferroelectrics and Frequency Control 57 (2010), pp. 654–668.
[30] J. Kuypers, L. Reindl, S. Tanaka, and M. Esashi, *Maximum accuracy evaluation scheme for wireless saw delay-line sensors*, IEEE Transactions on Ultrasonics, Ferroelectrics and Frequency Control 55 (2008), pp. 1640–1652.
[31] S. Kim, S. Carnes, A. Haldemann, E. Ng, and S. Arcone, *Miniature Ground Penetrating Radar, CRUX GPR*, in *IEEE Aerospace Conference*, Big Sky, MT, USA, 2006.
[32] J. Davis and A. Annan, *Ground penetrating radar for high resolution mapping of soil and rock stratigraphy*, Geophysical Prospecting 37 (1989), pp. 531–551.
[33] D. Rife and R. Boorstyn, *Single-Tone Parameter Estimation from Discrete-Time Observations*, IEEE Transactions on Information Theory IT-20 (1974), pp. 591–598.
[34] G. Hofbauer, *FMCW Based Readout System Accuracy Enhancement Techniques for Surface Acoustic Wave RFID sensors*, in *IEEE/MTT-S International Microwave Symposium*, Honolulu, HI, USA, 2007, pp. 575–578.
[35] S. Scheiblhofer, S. Schuster, M. Jahn, R. Feger, and A. Stelzer, *Performance Analysis of Cooperative FMCW Radar Distance Measurement Systems*, in *IEEE MTT-S International Microwave Symposium Digest*, Atlanta, GA, USA, 2008, pp. 121–124.

[36] J.M. Friedt, C. Droit, G. Martin, and S. Ballandras, *A wireless interrogation system exploiting narrowband acoustic resonator for remote physical quantity measurement*, Rev. Sci. Instrum. 81 (2010), p. 014701.

[37] D. Gachon, E. Courjon, G. Martin, L. Gauthier-Manuel, J.C. Jeannot, W. Daniau, and S. Ballandras, *Fabrication of High Frequency Bulk Acoustic Wave Resonator Using Thinned Single-Crystal Lithium Niobate Layers*, Ferroelectrics 362 (2010), pp. 30–40.